

Electron-loss cross sections, for 20-MeV Cl^{4+} and I^{5+} ions incident on thin gaseous targets: Experimental measurements and potential-model data analyses

H. A. Scott,* L. B. Bridwell,[†] C. D. Moak, G. D. Alton, C. M. Jones, P. D. Miller,
R. O. Sayer, Q. C. Kessel,[‡] and A. Antar[‡]

Oak Ridge National Laboratory, Oak Ridge, Tennessee 37830

(Received 21 July 1978)

Differential cross sections for charge change resulting from the scattering of 20-MeV $^{127}\text{I}^{5+}$ and 20-MeV $^{35}\text{Cl}^{4+}$ ions from thin gaseous targets have been measured. Total cross sections for multiple-electron loss have been determined by integration of the differential charge-state yields over angle. Cross sections are presented for $^{127}\text{I}^{5+}$ ions and $^{35}\text{Cl}^{4+}$ ions on Xe, Ar, and N_2 . Impact-parameter analyses of charge-fraction data have been performed; these analyses depend on the assumed interatomic potential but not on any absolute measurements. The applicability of Bohr, Thomas-Fermi, and Lenz-Jensen potentials was examined. The Bohr potential gave unsatisfactory fits to the directly measured cross sections for all observed collisions with impact parameters greater than about three times the screening radius. For the cases reported here, the Thomas-Fermi and Lenz-Jensen potentials tend to give underestimates of the total cross sections, probably because they do not take into account the ionized nature of the collisions partners.

I. INTRODUCTION

Charge-changing collisions of fast heavy ions with target atoms or molecules have recently received much attention as sources of information on interactions in complex atomic systems. Considerable effort has been devoted to measuring and calculating electron-capture and -loss cross sections. Detailed information is available from the angular distributions of the emergent charge states, which can be analyzed to give the impact-parameter dependence of the charge-changing events under single-collision conditions. A comprehensive review by Betz¹ contains theoretical and experimental results for total cross sections and charge-state distributions. Hahn² examined the angular distributions of individual charge states and the relative impact-parameter dependence of the charge-state distributions resulting from 15-MeV Ne and Ar ions scattered from thin gaseous targets and compared his findings with the theoretical predictions of Russek.³ These findings were not presented on an absolute basis and did not contain cross-section analyses. A recent theoretical treatment of charge-state distributions has been given by McGuire.⁴ Kessel,⁵ and later Spicuzza and Kessel,⁶ reported on collisions of I^{m+} incident on Xe, and Xe^+ incident on Xe at impact parameters in the range used in the present experiments. Their analysis dealt mainly with average charge-state values and used only the Bohr potential for impact-parameter analysis. Afrosimov *et al.*⁷ have reported some charge-state measurements for Kr^+ incident on Kr. For the multiple-scattering regime,⁸ we have measured charge-state angular distributions on an

absolute basis for 20-MeV I and Cl ions scattered from gaseous targets.

In this paper we use the classical correspondence between scattering angle and impact parameter to display the impact-parameter dependence of charge-state fractions and predict the total charge-changing cross sections. By comparing these cross sections with those obtained by direct integration of the absolute yields over angle, we obtain a sensitive test of the assumed interatomic potential. Cross sections are presented for 20-MeV $^{127}\text{I}^{5+}$ ions and $^{35}\text{Cl}^{4+}$ ions incident on Xe, Ar, and N_2 . The applicability of the Bohr, Thomas-Fermi, and Lenz-Jensen potentials is discussed.

II. APPARATUS

The experimental apparatus is virtually identical to that reported earlier.⁹ A momentum analyzed 20-MeV ion beam of either $^{127}\text{I}^{5+}$ or $^{35}\text{Cl}^{4+}$, produced in the Oak Ridge National Laboratory tandem accelerator, was collimated prior to entering a differentially pumped gas cell by two apertures, separated by 10 m, with diameters of 1.25 and 0.5 mm, respectively. The cell was positioned 27 cm after the second defining aperture and mounted directly above a 1400 L/sec diffusion pump; it consisted of two circular entrance apertures, each 1 mm in diameter, and two exit slot apertures 1×2.5 mm and 1×4 mm. All apertures were spaced 2 cm apart. The slotted exit apertures permitted observations of scattering at angles up to 3° . Target gases were introduced at the center of the gas cell. Charged particles scattered at a given angle were separated according to their charge with an electrostatic analyzer located approximately 3 m from the target.

III. CHARGE-STATE-FRACTION DATA AND ANALYSIS

In the charge-state analyzer a position sensitive detector was used to record charge-state distributions from which charge-state fractions $f_q(\theta_i)$ were derived (θ_i is the laboratory scattering angle). The acceptance solid angle, angular resolution, and charge-state resolution were determined by slits mounted in the electrostatic analyzer.

Total charge-changing cross sections $\sigma(q_i, q)$ can be obtained from the following expression

$$\sigma(q_i, q) = 2\pi \int_0^\infty f_q(p) p dp, \quad (1)$$

where $f_q(p)$ are the charge-state fractions as a function of impact parameter p . In order to analyze our data and perform this integration, it was necessary to substitute values of p for θ_i in the measured values of $f_q(\theta_i)$. The classical correspondence between center-of-mass scattering angle θ and impact parameter p for atomic scattering by a central potential $V(r)$ is given by¹⁰

$$\theta = \pi - 2 \int_{r_0}^\infty \frac{p/r^2}{[1 - p^2/r^2 - V(r)/E]^{1/2}} dr, \quad (2)$$

where E is the center-of-mass energy, r is the internuclear distance, and r_0 is the distance of closest approach. For a screened Coulomb potential of the form

$$V(r) = (Z_1 Z_2 e^2 / r) u(r/a), \quad (3)$$

where Z_1 and Z_2 are the atomic numbers of the colliding atoms, e is the electronic charge, u is the screening function, and a is the electronic screening length, it is possible to scale the collision parameters to produce a universal relation equivalent to Eq. (2) for all colliding atoms at nonrelativistic energies. Introducing the reduced

energy

$$\epsilon = (a/Z_1 Z_2 e^2) E \quad (4)$$

it follows that θ is a function of ϵ and p/a only. A perturbation treatment for small forward angles¹¹ shows that the reduced scattering angle $\bar{\theta} = \frac{1}{2}\epsilon\theta$ is a function of the parameter p/a alone. Universal relations between reduced scattering angle $\bar{\theta}$ and p/a for Rutherford scattering and three common screening functions, corresponding to Bohr, Thomas-Fermi, and Lenz-Jensen potentials have been calculated. The calculations for the Bohr potential, which are based upon the exponential screening function

$$u(r/a) = \exp(-r/a_B), \quad (5)$$

where

$$a_B = a_0 (Z_1^{2/3} + Z_2^{2/3})^{-1/2} \quad \text{and} \quad a_0 = 0.529 \times 10^{-8} \text{ cm}$$

were made using the method of Everhart *et al.*¹² The calculations with Thomas-Fermi and Lenz-Jensen potentials, where $a = 0.8853 a_B$, are due to Lindhard *et al.*¹¹

For each of the incident ion-target combinations used in the experiments reported here, the charge state fractions f_q were plotted as a function of impact parameter for cell pressures between 2 and 50 mTorr. The criterion for single-collision con-

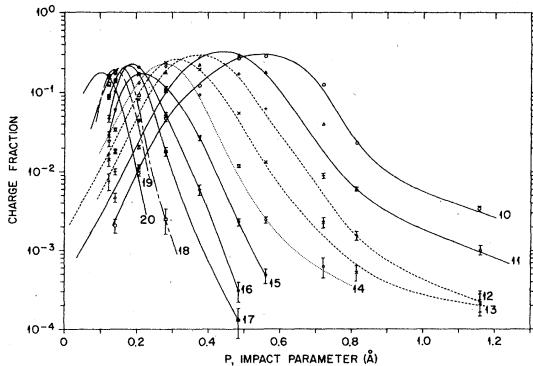


FIG. 1. Charge-state fractions vs Thomas-Fermi impact parameter for 20-MeV $^{127}\text{I}^{5+}$ incident on Xe (5-mTorr, 2-cm gas cell). $10 \leq q \leq 20$. Bars indicate statistical uncertainties.

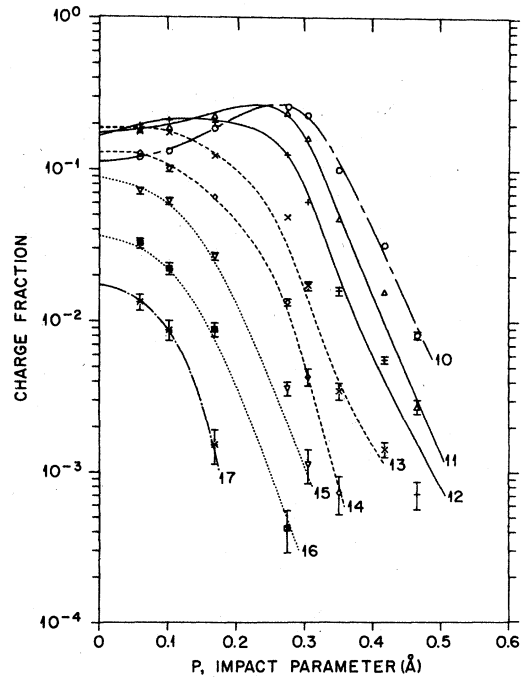


FIG. 2. Charge-state fractions vs Thomas-Fermi impact parameter for 20-MeV $^{127}\text{I}^{5+}$ incident on N_2 (10-mTorr, 2-cm gas cell). $10 \leq q \leq 17$. Bars indicate statistical uncertainties.

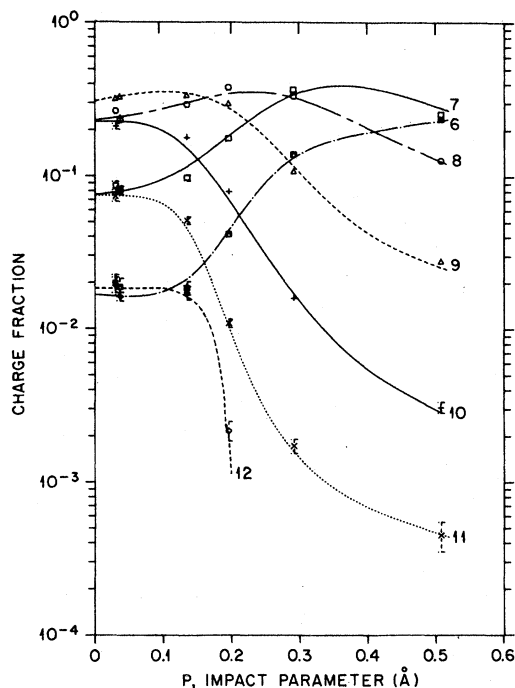


FIG. 3. Charge-state fractions vs Thomas-Fermi impact parameter for 20-MeV $^{35}\text{Cl}^{4+}$ incident on Ar (5-mTorr, 2-cm gas cell). $6 \leq q \leq 12$. Bars indicate statistical uncertainties.

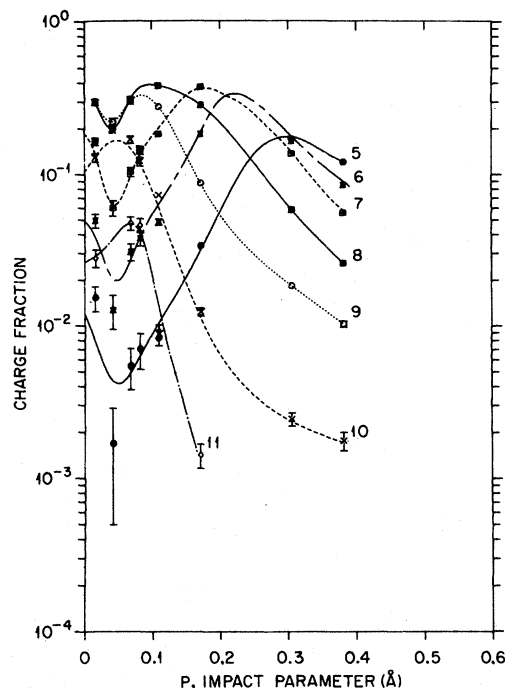


FIG. 4. Charge-state fractions vs Thomas-Fermi impact parameter for 20-MeV $^{35}\text{Cl}^{4+}$ incident on N_2 (5-mTorr, 2-cm gas cell). $5 \leq q \leq 11$. Bars indicate statistical uncertainties.

ditions is simply that the charge-state fractions obtained for an ion-target combination be identical, within experimental uncertainties, for the lowest cell pressures. Only the data satisfying this criterion were used in the analyses. Charge-state fractions resulting from 20-MeV $^{127}\text{I}^{5+}$ ions incident on Xe (5 mTorr) and N_2 (10 mTorr) are displayed in Figs. 1 and 2, respectively. Figures 3 and 4 present charge-state fractions resulting from 20-MeV $^{35}\text{Cl}^{4+}$ ions incident on Ar (5 mTorr) and N_2 (5 mTorr). The impact-parameter values used for the abscissas in Figs. 1-4 were determined by assuming a Thomas-Fermi potential. The resolutions in impact parameter corresponding to the angular resolutions used in the experiment were arranged so that the uncertainty in impact parameter was always less than 10% of the impact parameter and the vertical bars represent the statistical uncertainties.

IV. ABSOLUTE CHARGE-STATE YIELD DATA AND ANALYSIS

In order to obtain absolute differential charge-changing cross sections, incident-beam intensity, gas-target thickness, and solid-angle information are required. A surface barrier detector, used to detect particles multiply scattered at 60° from

a chemically etched annular Ni film situated between the two defining apertures, served as the incident-beam intensity monitor.¹³ Calibration of the monitor system provided a direct way of measuring the number of particles entering the target. Target pressures were measured with a capacitance manometer; cell pressures of 2-50 mTorr were used. The total charge-changing cross sections were determined by integrating the absolute yields over angle and employing the thin target relation

$$\sigma(q_i, q) = \frac{1}{Nt} \int Y_q(\Omega) d\Omega \quad \text{for } q \neq q_i, \quad (6)$$

where $Y_q(\Omega)$ is the measured absolute yield per incident particle per unit solid angle, N is the number density of the target gas, and t is the length of the gas cell. For absolute yield measurements, the single-collision criterion is that the yields increase linearly with target thickness and thus give constant cross-section values for the lowest target thicknesses. The range of target thicknesses for which this condition is met varies with the final charge state. Single-electron-capture cross sections $\sigma(q, q-1)$ have been found to increase sharply with ionic charge.¹ To avoid depletion of high-charge-state populations,

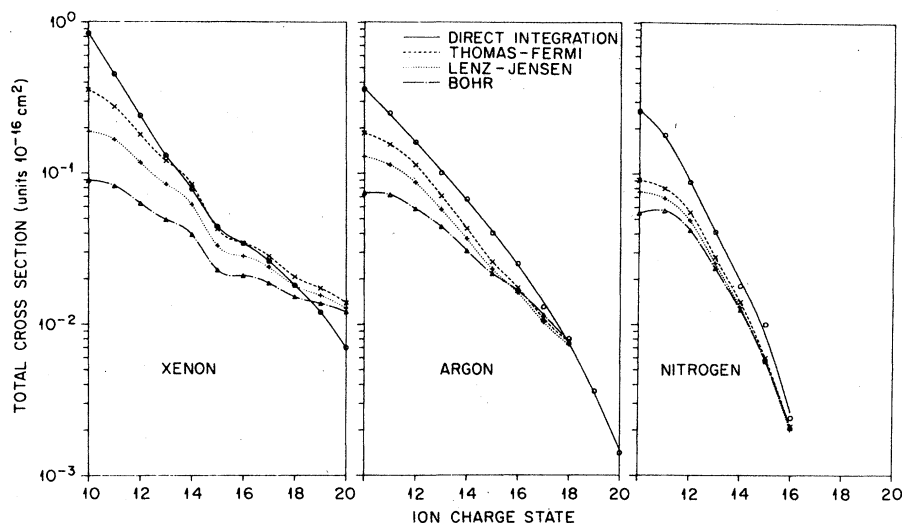


FIG. 5. Electron-loss cross sections $\sigma(5, q)$ for 20-MeV $^{127}\text{I}^{5+}$ on Xe, Ar, and N_2 . Symbols refer to means of determining cross sections. The open circles (O) were derived from the integration of measured absolute differential cross sections. Points were derived from Eq. (5) with Bohr (Δ), Thomas-Fermi (\times), and Lenz-Jensen ($+$), potentials. Lines are drawn to facilitate comparisons.

through electron capture after the initial collision in which the high charge states are produced, a thinner target is necessary than for low charge states. The experimentally determined cross sections $\sigma(q_i, q)$ for 20-MeV ^{127}I with $q_i = 5$ and 20-MeV ^{35}Cl with $q_i = 4$ remained constant to within $\sim 10\%$ for cell pressures up to 20 mTorr for $q < 15$, indicating that the single-collision criterion was satisfied. For $q \geq 15$ (only observed with ^{127}I), the onset of an apparent decrease in $\sigma(5, q)$ with pressure indicated where the single-collision criterion was not satisfied. Only data from the linear regions were used for cross-section calculations.

Figures 5 and 6 display the experimentally determined total cross sections $\sigma(q_i, q)$ for $^{127}\text{I}^{5+}$ and $^{35}\text{Cl}^{4+}$ incident ions, respectively. Each data point represents an average result over all cell pressures which fulfill the single-collision criterion.

ion. Cross sections calculated from charge-fraction data with Bohr, Thomas-Fermi, and Lenz-Jensen potentials are presented for comparison with the results obtained by direct integration of the absolute yields over angle.

V. DISCUSSION

Impact-parameter analyses for charge-changing collisions provide information on charge-changing processes which is not obtainable from total-cross-section measurements. High charge states are produced preferentially at small impact parameters, and the yield of the highest charge states also depends upon the collision partners and collision energy. The unexpected sharp increases in low-charge-state fractions (and decreases in high-charge-state fractions) at very small impact

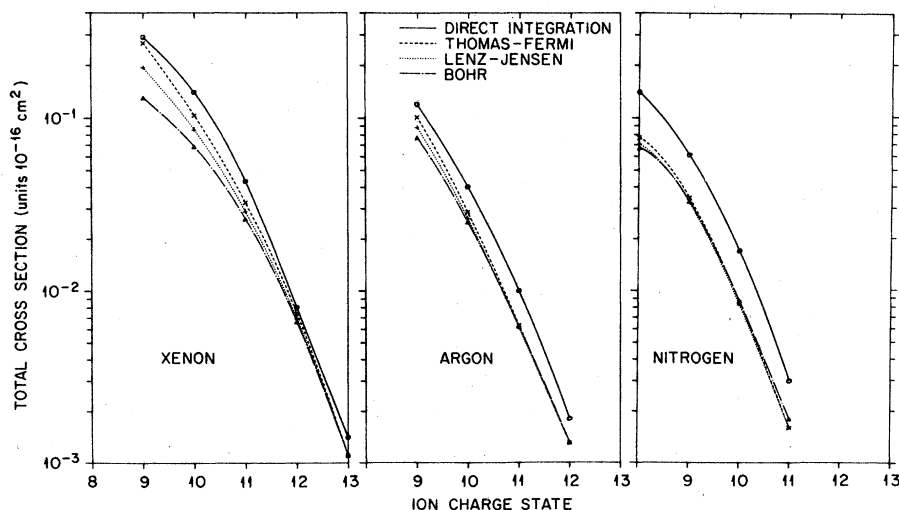


FIG. 6. Electron-loss cross sections $\sigma(4, q)$ for 20-MeV $^{35}\text{Cl}^{4+}$ on Xe, Ar, and N_2 . Symbols refer to means of determining cross sections. The open circles (O) were derived from the integration of measured absolute differential cross sections. Points were derived from Eq. (5) with Bohr (Δ), Thomas-Fermi (\times), and Lenz-Jensen ($+$) potentials. Lines are drawn to facilitate comparisons.

parameters ($p < 0.05 \text{ \AA}$) for ^{35}Cl incident on N_2 (Fig. 4) were also observed for ^{35}Cl incident on Ne, Ar, and Kr. Similar behavior was observed by Spicuzza and Kessel⁶ and is present in the data reported by Afrosimov *et al.*⁷ No complete explanation has been put forth, but presumably this effect is due to level promotions in the molecular orbital interactions although the effects seem to show little sensitivity to the choice of target. The additional data for Cl ions on Kr and Ne are omitted for the sake of brevity.

Although the Bohr potential has been used extensively for impact-parameter analyses, it is known to be unsatisfactory for collisions involving impact parameters larger than about 3 times the screening radius. The Thomas-Fermi and Lenz-Jensen interatomic potentials provide somewhat better descriptions. Both these potentials have been formulated for neutral collision partners, as noted by Knudsen.¹⁴ Examination of the curves shown in Figs. 5 and 6 indicates that the potentials used in processing the charge-fraction data tend to underestimate the total cross sections, especially for low charge states. In all cases, the Rutherford cross section is far above the mea-

sured values, so it seems that a potential which takes account of the fact that the interacting particles are not neutral could be made to fit the data. For example, in the case of I on Xe, the iodine ions have charge 5 and the Xe atom is neutral during approach but if the emerging iodine ion has charge state 15 it might be expected that the xenon atom would also be ionized to a comparable degree. Work is in progress to construct potentials which will give better agreement with the measured cross sections.

ACKNOWLEDGMENTS

The authors acknowledge with pleasure the assistance of W. T. Milner, E. G. Richardson, and R. P. Cumby and discussions with J. S. Briggs, H. Knudsen, and C. Bottcher. Special appreciation is expressed to G. A. Bazzell, R. F. Berkeley, J. E. Brockman, K. Z. Courtney, J. G. Crawford, M. J. Cullison, J. L. Godwin, and R. W. Walker for assistance in the data reduction. Research was sponsored by the Division of Physical Research, U. S. Department of Energy under Contract No. W-7405-eng-26 with Union Carbide Corporation.

*Graduate student from Cornell University, Ithaca, N. Y.

†Visiting scientist from Murray State University, Murray, Ky.

‡Visiting scientists from the University of Connecticut, Storrs, Conn.

¹H. D. Betz, *Rev. Mod. Phys.* **44**, 465 (1972).

²D. Hahn, *Winkelstreuung von Ne- und Ar-Ionen in "Gas Targets,"* Inaugural-Dissertation (der Freien Universität Berlin, 1976) (unpublished).

³A. Russek, *Phys. Rev.* **132**, 246 (1963).

⁴J. H. McGuire, *Phys. Rev. A* **9**, 286 (1974).

⁵Q. C. Kessel, *Phys. Rev. A* **2**, 1881 (1970).

⁶R. A. Spicuzza and Q. C. Kessel, *Phys. Rev. A* **14**, 630 (1976).

⁷V. V. Afrosimov, Yu. S. Gordeev, M. N. Panov, and N. V. Fedorenko, *Zh. Tekh. Fiz.* **36**, 123 (1977) [*Sov. Phys. Tech. Phys.* **11**, 89 (1966)].

⁸L. B. Bridwell, H. A. Scott, C. D. Moak, G. D. Alton, C. M. Jones, P. D. Miller, R. O. Sayer, Q. C. Kessel,

and A. Antar (unpublished).

⁹G. D. Alton, J. A. Biggerstaff, L. Bridwell, C. M. Jones, Q. Kessel, P. D. Miller, C. D. Moak, and B. Wehring, *IEEE Trans. Nucl. Sci.* **NS-22**, 1685 (1975).

¹⁰N. F. Mott and H. A. W. Massey, *The Theory of Atomic Collisions*, 2nd ed. (Oxford University, London, 1949), Chap. VII.

¹¹J. Lindhard, V. Nielsen, and M. Scharff, K. Dan. Vidensk. Selsk. Mat. Fys. Medd. **36**, 10 (1968).

¹²E. Everhart, G. Stone, and R. J. Carbone, *Phys. Rev.* **99**, 1287 (1955).

¹³B. R. Appleton, J. H. Barrett, T. S. Noggle, and C. D. Moak, *Radiat. Eff.* **13**, 171 (1972).

¹⁴H. Knudsen, "Experimental Studies of Small-Angle Multiple Scattering of Energetic Ions in Solid and Gaseous Targets," Ph.D. thesis (University of Aarhus, 1977) (unpublished).